Video-BM3D Denoising for BOTDA Sensing Systems

Biwei Wang,[1] Liang Wang,[2,*] Changyuan Yu,[1] and Chao Lu[1]
1 Department of Electronic and Information Engineering, The Hong Kong Polytechnic University, Kowloon, Hong Kong.
2 Department of Electronic Engineering, The Chinese University of Hong Kong, Shatin, N. T., Hong Kong.
**E-mail: cuhkwl@163.com*

Abstract: Video Block-Matching and 3D filtering (VBM3D) denoising has been demonstrated for the first time to improve the SNR in BOTDA, achieving 0.54MHz BFS uncertainty at the far end of 100.8km fiber with 2m spatial resolution.
OCIS codes: (060.2370) Fiber optics sensors; (290.5900) Scattering, Stimulated Brillouin; (190.4370) Nonlinear optics, fibers.

1. Introduction

Brillouin optical time domain analyzer (BOTDA) has attracted much interest over the past three decades due to its capability of distributed measurement of temperature/strain with excellent performance [1]. However, to achieve long sensing distance beyond 100km is a challenge since the signal-to-noise ratio (SNR) becomes worse at the far end of fiber due to the fiber attenuation. To extend the sensing range beyond 100km with acceptable spatial resolution and measurement accuracy, some methods have been proposed including optical pulse coding [2], Raman amplification [3], time/frequency-division multiplexing [4], random fiber laser amplification [5], Brillouin loss regime [6], and optical chirp chain BOTDA [7]. But most of the above methods require modifications of the conventional BOTDA setup which make the system complicated.

On the other hand, image denoising techniques have been used to improve the SNR without the need of modifying the conventional setup, such as non-local means (NLM) and wavelet denoising (WD) [8]. Recently we have proposed a novel Block-Matching and 3D filtering (BM3D) image denoising method to enhance the SNR [9]. BM3D combines the advantages of NLM and WD and hence shows less spatial resolution degradation and better measurement accuracy. However, 2D BM3D image denoising can only handle the situation that the environment condition is static and the measurand has no temporal evolution. In this paper, we extend the BM3D image denoising to video denoising, i.e. 3D Vedio-BM3D (VBM3D), in order to add one more temporal dimension and take the dynamical nature of environment into account. By using VBM3D denoising, the Brillouin frequency shift (BFS) uncertainty has been improved to be 0.54MHz for 100.8km sensing distance and 2m spatial resolution, which is the best accuracy achieved for 100km sensing distance.

2. BOTDA experiment setup

The BOTDA experiment setup shown in Fig. 1 is similar to that in Ref. [10]. The fiber under test (FUT) is 100.8km long single mode fiber. The last 196m loose fiber section is put in the oven to evaluate the measurement accuracy at the far end of the FUT. While another 2.3m loose fiber section is also kept inside the oven of 60ºC to verify the experimental spatial resolution. The rest of FUT is maintained at room temperature. 20ns pump pulse is used, corresponding to 2m spatial resolution. The pump peak power and the probe power injected into the FUT are 20dBm and -3dBm, respectively. A sampling rate of 500MSample/s and averaging times of 2000 are adopted for data collection on an oscilloscope .

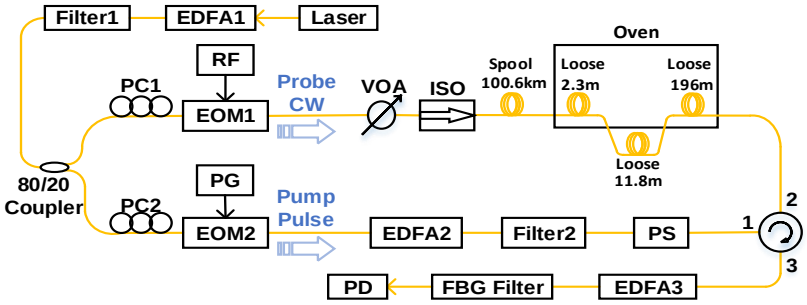

Fig. 1. BOTDA experiment setup. EDFA: erbium-doped fiber amplifier, PC: polarization controller, EOM: electro-optic modulator, RF: radio frequency, PG: pattern generator, VOA: variable optical attenuator, ISO: isolator, FUT: fiber under test, PS: polarization scrambler, FBG: fiber Bragg grating, PD: photodetector.

3. VBM3D denoising for BOTDA sensors

The flowchart of the proposed VBM3D denoising for BOTDA is shown in Fig. 2. Like 2D BM3D denoising, the VBM3D denoising also includes three main steps: grouping by block matching, collaborative filtering and aggregation [11]. Each 2D measurement of Brillouin gain spectrum (BGS) distribution along the FUT by the BOTDA system forms one frame of a video sequence, e.g. Frame 1, 2, 3 in Fig. 2. And multiple video frames are obtained by consecutive measurements and then are combined together to form the 3D video sequence, which will be denoised by VBM3D. In VBM3D the search range of block matching is 3D video sequences rather than 2D images as in BM3D, and the grouping is achieved by using predictive-search block-matching where some matched blocks "M" similar to the reference one "R" are searched and grouped together into a 3D array for each reference block in the video. Then the collaborative filtering includes 3D transformation and hard-threshold/Wiener filtering of the grouped 3D arrays. At last, the final estimates of the true video frames can be obtained by aggregation of all local estimates. For the collaborative filtering and aggregation, they are almost the same as those in BM3D [9].

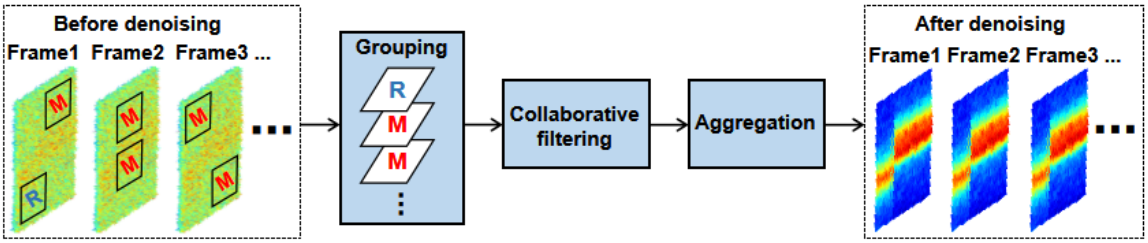

Fig. 2. Flowchart of the proposed VBM3D denoising for BOTDA. "M" and "R" represent the reference block and the matched ones.

In our experiment, 15 consecutive measurements of BGS distribution along the last 300m FUT have been taken to form a video sequence with maximum frame number of 15. Then the video is denoised by VBM3D. It is worth mentioning that the frame number determines the search range during block matching process and is a significant parameter in VBM3D algorithm. At first we set the frame number to be the maximum value of 15, which means that the block search range are the whole 15 measurements. Fig. 3(a) shows one of the 15 measured BGS distributions along the last 300m FUT, where the two heated sections can not be observed due to very low SNR at the FUT end.

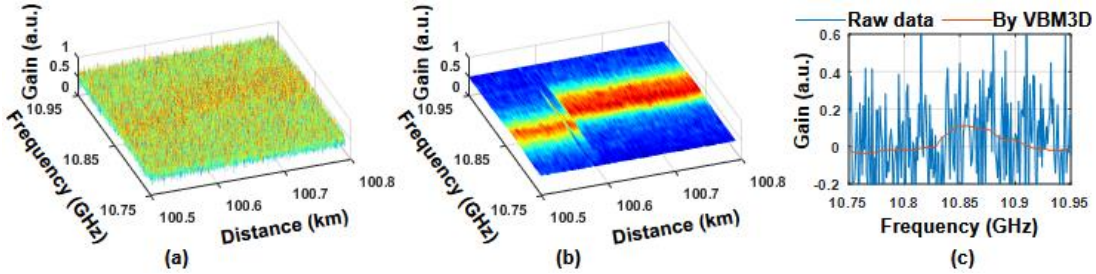

Fig. 3. (a) one of the 15 measured BGS distribution along the last 300m FUT before denoising; (b) the corresponding BGS distribution after denoising by using VBM3D with frame number of 15; (c) the corresponding BGS at the far end of FUT with/without denoising.

As a contrast, Fig. 3(b) gives the same BGS distribution after denoising by using VBM3D with frame number of 15, showing the two heated sections clearly at the FUT end. The BGSs at the FUT end in Fig. 3(a) and (b) are plotted in Fig. 3(c), implying that a clear local BGS can be reconstructed after denoising by VBM3D. By using Lorentzian curve fitting together with the temperature coefficient (1.034MHz/^{o}C) of the FUT, the corresponding temperature distribution is obtained, as shown in Fig. 4. It is obvious that the temperature fluctuations are reduced largely after denoising by VBM3D, and the temperature uncertainty at the far end of FUT is improved from 10.8^{o}C of raw data to 0.52^{o}C (0.54HMz BFS uncertainty) after denoising, as shown in Fig. 4(a). The temperature distribution around the

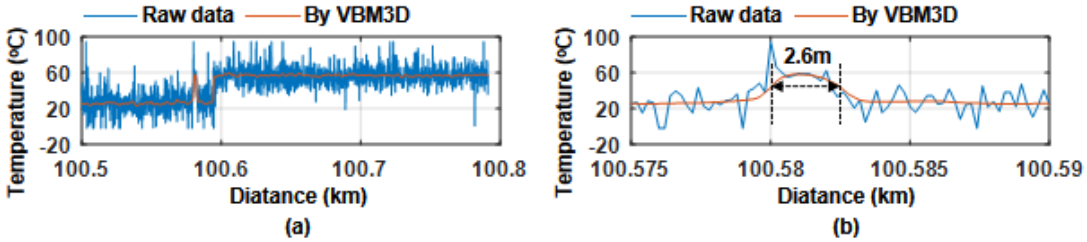

Fig. 4. Temperature distribution before and after denoising by using the VBM3D with frame number of 15: (a) along the last 300m FUT; (b) around the 2.3m heated section.

2.3m heated section in Fig. 4. (b) shows an experimental spatial resolution of 2.6m, indicating a very small degradation of spatial resolution after denoising. This result agrees well with our previous work of using BM3D denoising for BOTDA in Ref. [9].

Then we change the frame number in VBM3D algorithm and analyze the denoising performance. Fig. 5 shows the temperature uncertainty at the far end of FUT as a function of frame number, where the best temperature uncertainty among all of the frames used for denoising is adopted. When the frame number is 1, it means there is only one measurement and VBM3D works in the same way as 2D BM3D. The temperature uncertainty obtained by using VBM3D with frame number of 1, 2, 5, 10 and 15 are 2.13, 1.93, 1.38, 1.12 and 0.52°C, respectively. With increasing frame number, the temperature uncertainty decreases, indicating the superiority of the VBM3D over the BM3D that VBM3D can make use of not only the spatial correlation of the data within each frame but also the temporal correlation among different frames for denoising. Moreover, as a comparison we also give the temperature uncertainty obtained by using linear averaging of multiple measurements, as given in Fig. 5. The temperature uncertainty obtained using linear averaging of 1, 2, 5, 10 and 15 measurements are 9.0, 6.2, 4.1, 3.1 and 2.8°C, respectively. It can be seen that the temperature uncertainty obtained by VBM3D is much smaller than that by linear averaging, showing the capability of VBM3D to achieve signal denoising rather than averaging of redundant data.

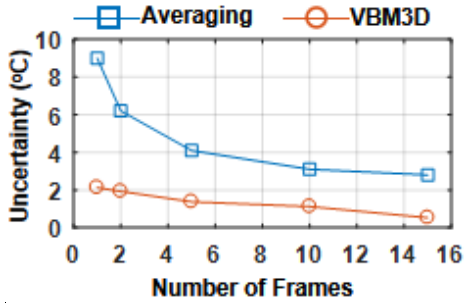

Fig. 5. Temperature uncertainty obtained by using VBM3D and linear averaging as a function of frame/measurement number.

4. Conclusions

We have proposed and demonstrated the use of VBM3D denoising to improve the measurement accuracy of BOTDA for the first time. By using 15 consecutive video frames for denoising, the BFS uncertainty of 0.54MHz has been achieved at the far end of 100.8km sensing fiber with 2m spatial resolution, which is the best accuracy achieved for fiber length beyond 100km. We believe VBM3D denoising would be helpful for long distance sensing, especially in dynamical environment.

Acknowledgement

Research Grants Council of Hong Kong projects: CUHK GRF 14204019; PolyU GRF 15211317.

References

[1] X. Bao, and L. Chen, "Recent progress in distributed fiber optic sensors," Sensors, **12**(7), 8601-8639 (2012).
[2] Z. Yang, M. A. Soto, and L. Thévenaz, "Increasing robustness of bipolar pulse coding in Brillouin distributed fiber sensors," Opt. Express 24, 586-597, 2016.
[3] M. A. Soto, X. Angulo-Vinuesa, S. Martin-Lopez, S. H. Chin, J. D. Ania-Castanon, P. Corredera, E. Rochat, M. Gonzalez-Herraez, and L. Thevenaz, "Extending the real remoteness of long-range Brillouin optical time-domain fiber analyzers," Journal of Lightwave Technology, 32(1): 152-162, 2014.
[4] Y. Fu, Z. Wang, R. Zhu, N. Xue, J. Jiang, C. Lu, B. Zhang, L. Yang, D. Atubga, and Y. Rao, "Ultra-long-distance hybrid BOTDA/φ-OTDR," Sensors, **18**(4), 976 (2018).
[5] Fu, Yun, R. Zhu, B. Han, H. Wu, Y. Rao, C. Lu, and Z. Wang, "175km repeaterless BOTDA with hybrid high-order random fiber laser amplification." Journal of Lightwave Technology, DOI: 10.1109/JLT.2019.2916413 (2019).
[6] J. J. Mompó, J. Urricelqui, and A. Loayssa, "Brillouin optical time-domain analysis sensor with pump pulse amplification," Opt. Express 24, 12672-12681, 2016.
[7] B. Wang, B. Fan, D. Zhou, C. Pang, Y. Li, D. Ba, and Y. Dong, "High-performance optical chirp chain BOTDA by using a pattern recognition algorithm and the differential pulse-width pair technique," Photon. Res. 7, 652-658, 2019.
[8] M. A. Soto, J. A. Ramírez, and L. Thévenaz, "Intensifying the response of distributed optical fibre sensors using 2D and 3D image restoration," Nat. Commun. **7**: 10870 (2016).
[9] H. Wu, L. Wang, Z. Zhao, N. Guo, C. Shu, and C. Lu, "Brillouin optical time domain analyzer sensors assisted by advanced image denoising techniques," Optics express 26.5: 5126-5139 (2018).
[10] B. Wang, L. Wang, N. Guo, Z. Zhao, C. Yu, and C. Lu, "Deep neural networks assisted BOTDA for simultaneous temperature and strain measurement with enhanced accuracy," Optics express, 27(3): 2530-2543 (2019).
[11] K. Dabov, A. Foi, and K. Egiazarian, "Video denoising by sparse 3D transform-domain collaborative filtering," in Proc. European Signal Processing Conference (EUSIPCO) (IEEE, 2007), Poznan, paper 145-149 (2017).